J Mater Sci (2007) 42:1751–1756
DOI 10.1007/s10853-006-0822-0

Abnormal strain hardening in nanostructured titanium at high strain rates and large strains

Y. M. Wang · J. Y. Huang · T. Jiao · Y. T. Zhu · A. V. Hamza

Received: 22 May 2006 / Accepted: 18 August 2006 / Published online: 16 December 2006

Abstract Commercial purity nanostructured titanium prepared by equal channel angular pressing plus cold rolling (grain size ~260 nm) exhibits a nonnegligible strain hardening behavior at large compressive strains (>15%) and quasistatic loading conditions. The degree of the strain hardening increases with increasing strain rates and becomes more pronounced at dynamic loading rates. This behavior is in contrast with what we have seen so far in other nanostructured materials, where flat stress-strain curves are often seen. It was concluded from transmission electron microscopy investigations that in addition to dislocation slips, deformation twinning may have played a significant role in plastic deformation of nanostructured Ti. The structural failure behavior is in-situ recorded by a CCD camera and reasoned according to the microscopic observations.

Y. M. Wang (✉) · A. V. Hamza
Chemistry and Materials Science Directorate, Lawrence Livermore National Laboratory, 7000 East Ave., Livermore, CA 94550, USA
e-mail: ymwang@llnl.gov

J. Y. Huang
Department of Physics, Boston College, Chestnut Hill, MA 02467, USA

T. Jiao
Department of Mechanical Engineering, Brown University, Providence, RI 02912, USA

Y. T. Zhu
Materials Science and Technology Division, Los Alamos National Laboratory, Los Alamos, NM 87545, USA

Introduction

Hexagonal close-packed (hcp) ultrafine-grained (UFG) titanium processed by severe plastic deformation (SPD) has gained wide interest due to its excellent mechanical properties and potential applications as biomedical implants [1–3]. Unlike traditional fcc and bcc nanostructured materials, the nanostructured titanium prepared by SPD contains not only high densities of dislocations but also a significant amount of deformation twins. Such unique microstructural characteristic suggests that the deformation mechanism and failure mode of nanostructured Ti may be different from those of other UFG materials. It is well-established that deformation twinning is an important mode of deformation in coarse-grained hcp materials. Whether and when dislocation slip or deformation twinning becomes the dominant deformation mode in nanostructured Ti remain an open question.

To date, a large amount of work [1–8] has been reported on the deformation behavior and failure mechanism of nanocrystalline and UFG materials, the bulk of which has focused on fcc and bcc crystal structures. Quite different deformation modes were documented for these two types of nanostructured materials. SPD nanostructured Cu (fcc), for example, shows near perfect elasto–plastic behavior under both compression and tension, with a total compressive strain over 70% [9, 10]. Deformation twinning was not observed in this material except at low deformation temperatures or under high-pressure torsion condition [2, 11]. On the other hand, hot-consolidated bcc nanostructured Fe, though also showing a near elastic-perfectly plastic behavior at small compressive strains (<10%), fails prematurely due to the development of

multiple shear bands that are attributed to the diminishing strain hardening and strain rate hardening capability [12]. Earlier studies of nanostructured Ti at different strain rates suggested that similar to nanostructured Fe, UFG-Ti also exhibited a reduced strain hardening behavior. However, no microstructural evolution and damage mechanisms were reported [1].

In this study, we extend the mechanical testing of nanostructured Ti to much larger strains and a wide range of strain rates in order to understand what factors and how they control the deformation/failure behavior of UFG-Ti. We paid special attention on the possibility of twinning activities in nanostructured Ti that were previously overlooked. In order to do so, the mechanical properties of nano-Ti were systematically characterized. An in-situ high speed camera was employed in the experiments so as to capture the evolution of surface micrographs in UFG-Ti during dynamic compressions. The postmortem microstructures at different strains were examined by transmission electron microscopy (TEM). The results were used to interpret the deformation mechanism and failure mode of UFG-Ti.

Experimental

Ultrafine-grained Ti was produced by equal channel angular pressing (ECAP) of commercial purity titanium (0.12%O, 0.07%C, 0.04%N, 0.01%H, 0.18%Fe, and balanced Ti) following route B_c for eight passes at 400–450 ^{o}C. The workpieces were further processed by cold rolling at room temperature to a total cross-sectional area reduction of 73%. The details of the processing method were given in reference [2]. The as-rolled microstructures show grains elongated along the longitudinal rolling direction and near equal-axial in the transverse cross section. The reference coarse-grained (CG) Ti was prepared by annealing a commercial Ti (99.9%) at 705 ^{o}C for 2 h and then air-cooling, resulting in an average grain size of 35 μm. Before the mechanical testing, the nanostructured samples were sit at room temperature for over a year.

The specimens for quasistatic and dynamic compression tests were cut (with the mechanical testing axis parallel to the ECAP longitudinal direction) from the as-processed samples using an Electrical-Discharging-Machine (EDM). Then the side surfaces of the specimens were polished using SiC abrasive papers with metallurgical grits down to 1,200 and diamond paste of 0.1 μm. To ensure the parallelism of the two loading surfaces, the specimens were mounted into epoxy and the loading surfaces were lapped using a LapMaster lapping machine with an Accupol to remove the rough layers. After lapping, the flatness of the two ground surfaces was less than 1 μm/30 mm. The dimensions of the specimens were 2.5 mm × 2.5 mm × 3.5 mm and ϕ3 mm × 2.4 mm for quasistatic and high strain rate compression tests, respectively. In order to record the potential development of cracking or shear banding on the sample surfaces during dynamic loading, a prismatic side surface was cut for cylindrical samples and polished down to 0.1 μm finish for in-situ imaging during the dynamic loading experiments.

The quasistatic compression tests were carried out using a MTS servo-hydraulic machine under a constant displacement control mode with initial strain rates of 10^{-4} s^{-1}–10^{-1} s^{-1}. The interface between the specimens and the compression platens was lubricated by lithium complex grease to reduce the influence of interfacial friction. The dynamic compression tests were performed using the Kolsky bar technique (Split Pressure Hopkinson Bar) at the strain rates of 10^{3} s^{-1}–10^{4} s^{-1}. A high speed camera (DRS ULTRA 8) having the capacity to catch consecutive pictures at every 2 ms was used to in-situ record the surface micrographs of the samples during the dynamic tests. For each stress-strain curve reported here, at least two tests were carried out in order to verify the reproducibility.

The deformed UFG-Ti samples were sectioned parallel to the compression axis and characterized by transmission electron microscopy (TEM), which was conducted in a JEOL 3000 FEG electron microscope operated at 300 kV. TEM samples were prepared by double-jet electro-polishing at room temperature with an electrolyte consisting of 33% orthophoshporic acid and 67% water.

Results and discussions

Figure 1 shows true stress-strain curves of UFG-Ti with the strain rate in the range of 10^{-4} s^{-1}–10^{-1} s^{-1}. For comparison, the stress-strain curve of a coarse-grained (CG) Ti is also included. A considerably elevated strength was observed in UFG-Ti with the yield stress 3–4 times higher than that of CG-Ti. In terms of ductility, UFG-Ti fails after a total compressive strain of ~30%, as compared to ~60% in CG-Ti and ~10% in nanostructured Fe [12]. Such ductility is consistent with what we have seen so far in other nanostructured metals, where a notable reduction of tensile/compressive strain to failure was observed as a result of nanostructuring.

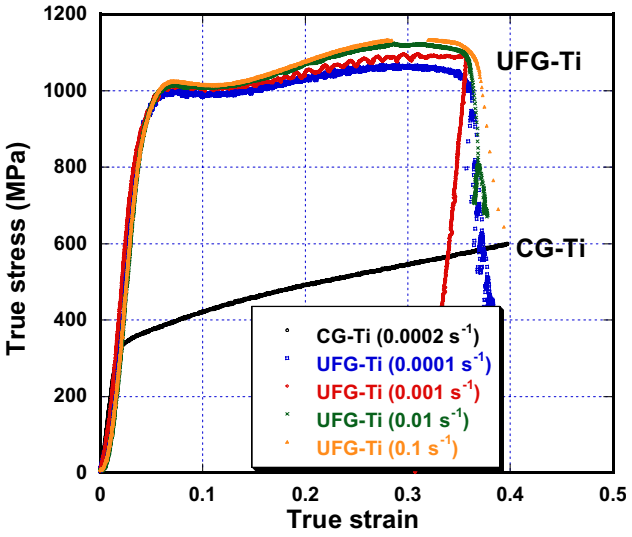

Fig. 1 Room temperature compressive true stress-strain curves of nanostructured Ti over strain rate range of 10^{-4} s^{-1}–10^{-1} s^{-1}, in comparison with a representative true stress-strain curve of the coarse-grained Ti. Only first 40% plastic strain is shown for coarse-grained Ti

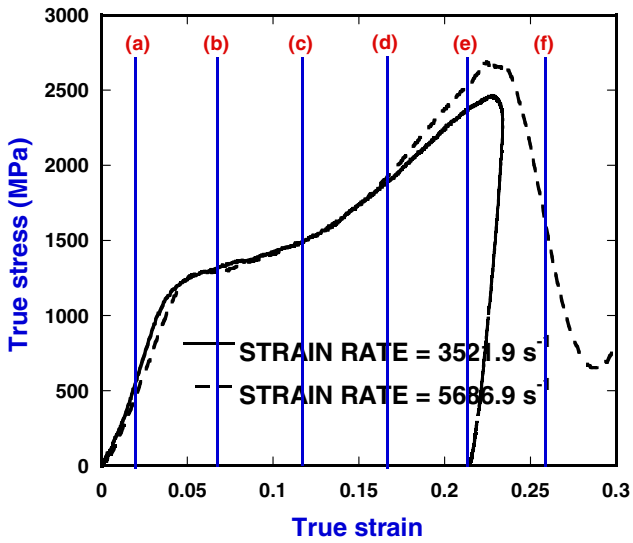

Fig. 2 Dynamic compressive true stress-strain curves of nanostructured Ti at room temperature

Careful examinations of the strain hardening behavior in UFG-Ti and CG-Ti reveal distinctive differences. The CG-Ti demonstrates a strong strain hardening behavior, the stress-strain curve of which has a perceptible upward curvature throughout the test. Such an increasing strain hardening behavior in CG-Ti is believed to be associated with extensive twinning, as documented by Chichili [13] and Harding [14]. In contrast, a different scenario is observed for the plastic flow of UFG-Ti, which exhibits initially little strain hardening, with a near perfectly plastic behavior at strains up to 15%. This low strain hardening behavior at small strains agrees with our previous observations and is believed to render early tensile instability in nanostructured Ti [1]. At large strains, however, a nonnegligible strain hardening is observed (Fig. 1), though the degree of such strain hardening remains limited and far less than that of CG-Ti.

The strain hardening for UFG-Ti becomes more pronounced when the samples were tested at high strain rates, as shown in Fig. 2. This strain hardening behavior appears fairly reproducible in our multiple tests of different geometry samples. Note that the specimen-platen interface was sufficiently lubricated during all the compression tests such that the optical micrographs of the deformed samples showed no evidence of inhomogeneous flow or barreling. Therefore the observed strain hardening behavior reflects the intrinsic material behavior, and its variation with strain and strain rate is related to the microscopic deformation mechanism of UFG-Ti. Such a strong increased strain hardening behavior has not been reported in other ultrafine-grained materials and is clearly worthy of further investigations.

Figure 3 displayed sequential TEM bright field images of the as-processed and deformed UFG-Ti. Due to the cold-rolling procedure, many grains in the as-prepared samples exhibit filamentary shapes along the longitudinal rolling direction (Fig. 3a), with an average grain size of ~260 nm. Dislocation cells and extremely high density of dislocations are the typical microstructural features. Deformation twins resulted from severe plastic deformation are also visible inside grains with the twin band width on the order of ~150 nm. After 10% deformation (Fig. 3b), the ultrafine-grains become more or less equiaxed, though some grains with straight boundaries and elongated contours are still observable. The average grain size remains approximate constant across the transverse direction. After 30% strain (Fig. 3c), the grains look completely equal-axed (the sample failed at this point). The transformation of grain shape from fibrous type to equal-axial type during the quasistatic compressions implies the change of grain orientations and evolution of the texture, suggesting that the dislocation slip plays a significant role during plastic deformation of UFG-Ti [2]. Mechanical twinning is known to strongly affect the deformation behavior of coarse-grained hcp materials. Interestingly, our TEM examinations in quasistatic deformed samples revealed little evidence of additional twinning activities except at very large strains. This supports the notion that dislocation slip is the major mode of deformation in nanostructured Ti at slow deformation rates and room temperature [2].

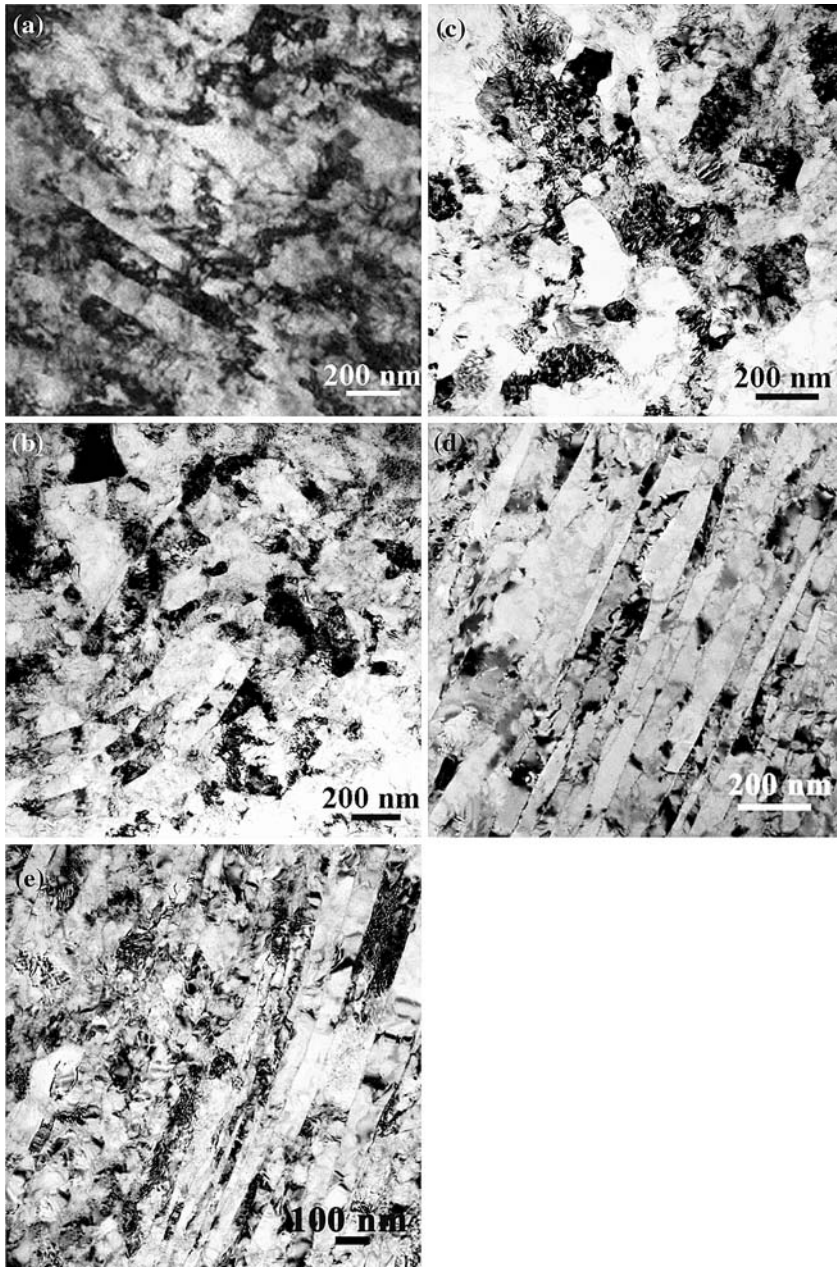

Fig. 3 TEM bright-field images of (**a**) as-processed, (**b**) 8%, (**c**) 30%, (**d**) high strain rate, and (**e**) low-temperature (77 K) deformed UFG-Ti

At dynamic loading rates (10^3–10^4 s^{-1}), however, a different scenario is observed, Fig. 3d. Deformation twin with the band width in the range of 50–100 nm become the characteristic microstructural feature. Note that the twin bands in as-processed samples are noticeably wider, suggesting that deformation twinning has become an important event during high strain rate deformation of UFG-Ti. Additional and extensive twinning activities were also observed when nanostructured Ti was deformed at cryogenic temperature (77 K) [15], as shown in Fig.3e. It is noticed that the twin bands observed in low-temperature deformation is narrower (in the range of 10–50 nm) than those seen at high strain rates. This indicates that the twinning activity in nanostructured Ti is closely tied to deformation conditions such as strain rates and temperatures. The lack of significant twinning activity at slow strain rates is not surprising, considering that the as-prepared materials contain a high density of mobile dislocations and/or deformation twins.

In addition to deformation twinning, it was suggested by Nemat-Nasser et al. [16] that the dynamic strain aging effect in commercial purity Ti should also be taken into account when discussing the strain hardening behavior of hcp Ti. Such dynamic strain hardening is believed to be caused by the interaction

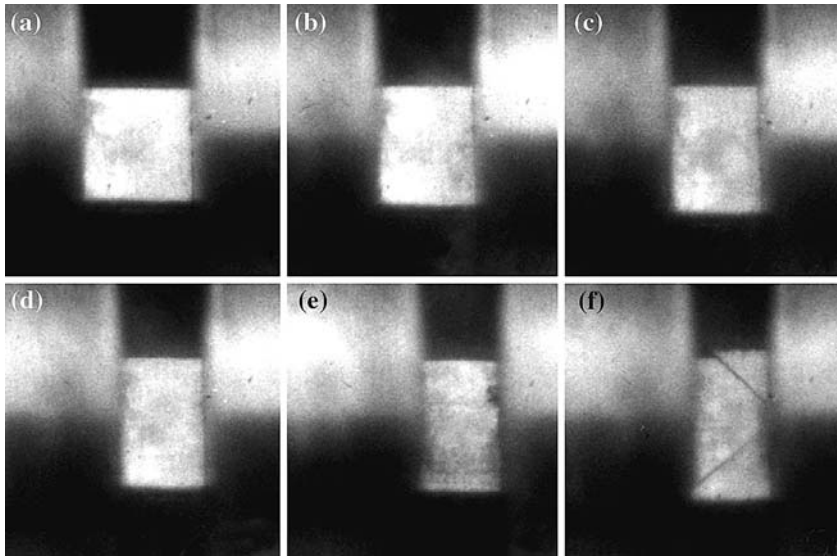

Fig. 4 (**a**)–(**f**) In situ high speed camera pictures of UFG-Ti during a dynamic compression test. Note the development of cracks with increasing strains

between moving dislocations and solute atoms. Nemat-Nasser et al. proposed that the dynamic strain aging is due to the directional diffusion of dislocation-core point defects with the moving dislocations at high strain rates, although the usual dynamic strain aging by point defects segregating outside the dislocation core through volume diffusion is also possible at low strain rates. Because of the diffusion mechanism involved, however, the dynamic strain aging generally occurs at elevated temperatures (600–850 K). Therefore it is expected that such dynamic strain aging has little implication on the strain hardening behavior seen in our experiments.

The strain hardening behavior has direct impact on the failure mode of UFG-Ti. The development of cracks during dynamic testing was captured by a high speed camera and shown in Fig. 4. The alphabetic order of the pictures is the same as those marked on the stress-strain curve of UFG-Ti (Fig. 2) with each letter representing a different strain level. The time interval between two frames is 10 ms, and the camera exposure time for each image is 1 ms. Note that the cracks started to develop in the late stage of deformation (Fig. 4f), i.e., sudden strain hardening regime), where the substantial strain hardening has advanced. Though shear banding or surface roughing due to dislocation slip or grain boundary sliding was not captured by the high speed camera, postmortem optical micrographs (not shown) revealed that local microscopic shearing did occur in nanostructured Ti, but no large shear bands were formed and penetrated through the whole sample. The strong strain hardening during the late stage of deformation apparently froze the occasional shear localizations. Close examinations of the fracture micrographs of the samples after quasistatic compressions showed that cracks were initiated from either the corner of the top surface or the bottom surface and propagated to the opposite direction (see Fig. 4f). The multiple shear bands were not detected during the compression, suggesting overall homogenous deformation nature of the UFG-Ti. These observations imply that the initialization and development of the cracks are likely due to the continuous increase of the flow stress, which eventually reaches over the critical shear stress level that ruptures the UFG-Ti samples. Such failure behavior bears similarity to those observed in ductile coarse-grained polycrystalline materials [17], but is somewhat different from those reported in other UFG materials.

Summary

The mechanical behavior of ultrafine-grained titanium has been investigated by compression tests over a wide strain rate range of 10^{-4} s^{-1}–10^{4} s^{-1}. The flow stress of UFG-Ti showed an abnormal strain hardening behavior at large strains and dynamic loading rates. The onset of such abnormal strain hardening behavior can be associated with twinning activities instead of dynamic strain aging in nanostructured Ti. No plastic instability or grain-boundary-related mechanism was observed during the compression of UFG-Ti. As a result, nanostructured Ti shows a different failure mode in compared with other ultrafine-grained materials.

Acknowledgements YMW thanks Prof. Ma at Johns Hopkins University for his early supports and inspiring discussions. TJ is indebted to Prof. Ramesh for the access of dynamic loading

facilities. The work at Lawrence Livermore National Laboratory was performed under the auspices of the U.S. Department of Energy under contract No. W-7405–Eng-48.

References

1. Jia D, Wang YM, Ramesh KT, Ma E, Zhu YT, Valiev RZ (2001) Appl Phys Lett 79:611
2. Zhu YT, Huang JY, Ungar T, Wang YM, Ma E, Valiev RZ (2003) J Mater Res 18:1908
3. Sergueeva V, Stolyarov VV, Valiev RZ, Mukherjee AK (2001) Scr Mater 45:747
4. Stolyarov VV, Zhu YT, Lowe TC, Valiev RZ (2001) Mater Sci Eng A303:82
5. Wang YM, Ma E, Chen MW (2002) Appl Phys Let 80:2395
6. Wang YM, Chen MW, Zhou FH, Ma E (2002) Nature 415:912
7. Chinh NQ, Szommer P, Horita Z, Langdon TG (2006) Adv Mater 18:34
8. Wang YM, Hodge AM, Biener J, Hamza AV, Barnes DE, Liu K, Nieh TG (2005) Appl Phys Lett 86:101915
9. Valiev RZ, Kozlov EV, Ivanov YF, Lian J, Nazarov AA, Baudelet B (1994) Acta Metall Mater 42:2467
10. Wang YM, Ma E (2004) Acta Mater 52:1699
11. Liao XZ, Zhao YH, Srinivasan SG, Zhu YT, Valiev RZ, Gunderov DV (2004) Appl Phys Lett 84:592
12. Jia D, Ramesh KT, Ma E (2003) Acta Mater 51:3495
13. Chichili DR, Ramesh KT, Hemker KJ (1998) Acta Mater 46:1025
14. Harding J (1975) Archives Mech 27:715
15. Wang YM, Ma E, Valiev RZ, Zhu YT (2004) Adv Mater 16:328
16. Nemat-Nasser S, Guo WG, Cheng JY (1999) Acta Mater 47:3705
17. Hertzberg RW (1995) Deformation and fracture mechanics of engineering materials. 4th edn. New York, John Wiley and Sons p 344